2-16-2001

Ice Nucleation in Sulfuric Acid and Ammonium Sulfate Particles

Anthony J. Prenni
University of Colorado, Boulder

Matthew E. Wise
University of Colorado, Boulder, mawise@cu-portland.edu

Sarah D. Brooks
University of Colorado, Boulder

Margaret A. Tolbert
University of Colorado, Boulder

JOURNAL OF GEOPHYSICAL RESEARCH, VOL. 106, NO. D3, PAGES 3037-3044, FEBRUARY 16, 2001

Ice nucleation in sulfuric acid and ammonium sulfate particles

Anthony J. Prenni,[1] Matthew E. Wise, Sarah D. Brooks, and Margaret A. Tolbert
Department of Chemistry and Biochemistry and CIRES, University of Colorado, Boulder

Abstract. Cirrus clouds are composed of ice particles and are expected to form in the upper troposphere when highly dilute sulfate aerosols cool and become supersaturated with respect to ice. In the laboratory we have used Fourier transform infrared spectroscopy to monitor ice nucleation from sulfate particles for relevant compositions of sulfuric acid/water and ammonium sulfate/water aerosols. Measured freezing temperatures are presented as a function of aerosol composition, and results are compared to existing aerosol data. We find that sulfuric acid solution aerosol exhibits greater supercooling than ammonium sulfate solution aerosol of similar weight percent. Ice saturation ratios based on these measurements are also reported. We find that ammonium sulfate solution aerosol exhibits a relatively constant ice saturation of S~1.48 for ice nucleation from 232 to 222 K, while sulfuric acid solution aerosol shows an increase in ice saturation from S~1.53 to S~1.6 as temperature decreases from 220 K to 200 K. These high-saturation ratios imply selective nucleation of ice from sulfate aerosols.

1. Introduction

Sulfate aerosols are abundant throughout the upper troposphere and are thought to play a significant role in heterogeneous chemistry [*Hu and Abbatt*, 1997; *Lary et al.*, 1997], climate forcing [*Charlson et al.*, 1992; *Pandis et al.*, 1995], and cirrus cloud formation [*DeMott and Rogers*, 1990; *Sassen and Dodd*, 1988; *Tabazadeh et al.*, 2000]. Cirrus clouds, in turn, play a dual role in the Earth's radiation budget, increasing the Earth's albedo while simultaneously decreasing emission of infrared radiation to space. It is believed that these combined effects cause a net warming at the Earth's surface. Cirrus clouds may also play a role in heterogeneous chemistry in the upper troposphere, particularly in midlatitude ozone depletion [*Solomon et al.*, 1997]. Determining the conditions under which cirrus clouds form is thus essential for accurate modeling of climate and chemistry in the atmosphere.

It is thought that cirrus clouds form naturally in the upper troposphere when highly dilute sulfate aerosols cool and become supersaturated with respect to ice. These particles can then homogeneously nucleate ice to form cirrus particles. Bulk studies have been performed to study the formation of ice in binary sulfuric acid and water solutions [*Gable et al.*, 1950; *Ohtake*, 1993; *Zhang et al.*, 1993]. However, aerosol particles are known to supercool due to their small size. To determine formation conditions for cirrus particles it is thus essential to use appropriately sized particles for freezing measurements in the laboratory. *Imre et al.* [1997] used a single-particle levitation technique to measure phase transitions of individual H_2SO_4/H_2O particles. *Martin et al.* [1997] measured ice nucleation from sulfuric acid solution particles deposited on a gold surface. For both of these studies, however, ice supersaturation conditions were not attainable. *Bertram et al.* [1996] studied submicrometer H_2SO_4/H_2O aerosols using a low-temperature flow tube system. In their system, ice supersaturations were readily attainable at tropospheric temperatures, and ice formation was measured as a function of aerosol composition. *Clapp et al.* [1997] also used Fourier transform infrared spectroscopy to measure ice nucleation in H_2SO_4/H_2O aerosol. Their results for the onset of ice nucleation are in good agreement with the studies of *Bertram et al.* [1996]. *Koop et al.* [1998] have recently investigated the freezing of H_2SO_4/H_2O particles larger than 1 μm in diameter on a hydrophobic plate using an optical microscope. Their results indicate significantly lower freezing temperatures than those reported by *Bertram et al.* [1996] for comparable aerosol compositions. More recent studies [*Cziczo and Abbatt*, 1998; *Chen et al.*, 2000] have determined freezing temperatures that are even lower than those reported by *Koop et al.* [1998].

In addition to ice nucleation from binary H_2SO_4/H_2O, cirrus clouds may nucleate from ammonium sulfate aerosols. Recent measurements by *Talbot et al.* [1998] indicate that NH_4^+ is often present in upper tropospheric aerosol. *Tabazadeh and Toon* [1998] and *Martin* [1998] suggest that the presence of ammonium ions in sulfate-based aerosol may influence the occurrence of cirrus clouds in the upper troposphere. A number of groups have investigated the deliquescence and efflorescence behavior of ammonium sulfate [*Cziczo and Abbatt*, 1999; *Onasch et al.*, 1999; *Xu et al.*, 1998]. While ammonium sulfate may exist as a solid in the atmosphere, these studies indicate that relatively dry conditions are necessary for efflorescence of submicrometer particles at atmospheric temperatures. Therefore ammonium sulfate will probably exist as a solution under many atmospheric conditions.

Numerous studies have been done on the formation of ice from bulk ammonium sulfate solutions [see *Timmermans*,

[1]Now at Colorado State University, Department of Atmospheric Science, Fort Collins, Colorado.

Paper number 2000JD900454.
0148-0227/01/2000JD900454$09.00

1960]. Recently, *Xu et al.* [1998] investigated the ice-solution equilibrium line of $(NH_4)_2SO_4$ using the single-particle levitation technique. To reach supersaturated conditions, *Cziczo and Abbatt* [1999] used a flow tube system to study the formation of ice in $(NH_4)_2SO_4/H_2O$ aerosol over a broad range of compositions. Their data indicate that atmospheric aerosol composed of ammonium sulfate solution can nucleate ice at a much higher temperature than sulfuric acid particles of similar weight percent. A new FTIR aerosol study by *Chelf and Martin* [2000] reports freezing temperatures for ammonium sulfate solutions similar to those of *Cziczo and Abbatt* [1999]. *Bertram et al.* [2000] have used differential scanning calorimetry and optical microscopy to measure ice nucleation in ammonium sulfate aerosol. They observed much greater supercooling than reported by *Cziczo and Abbatt* [1999]. Finally, *Chen et al.* [2000] have measured ice nucleation from ammonium sulfate aerosol using a continuous flow thermal diffusion chamber. Their results fall between those found by *Cziczo and Abbatt* [1999] and *Bertram et al.* [2000].

Despite the abundance of aerosol data for ice formation from sulfuric acid and ammonium sulfate solution aerosol, there are large discrepancies in the reported freezing temperatures. In an attempt to determine the most appropriate values for ice nucleation parameters in cirrus cloud models, we have measured ice nucleation in submicrometer H_2SO_4/H_2O and $(NH_4)_2SO_4/H_2O$ aerosols using Fourier transform infrared (FTIR) spectroscopy in a temperature-controlled flow tube system. FTIR spectroscopy has proven effective for measuring ice nucleation in sulfate aerosol [*Bertram et al.*, 1996; *Cziczo and Abbatt*, 1999]. We deviate from earlier FTIR studies, however, in our method of determining aerosol composition. Rather than using an infrared calibration for determining the particle composition, we have designed a method for conditioning our aerosol to a known, desired concentration. This method has resulted in freezing point measurements which differ somewhat from FTIR aerosol studies but which are consistent with results of ice nucleation from studies using the other experimental techniques listed above.

2. Experiment

2.1. Sulfuric Acid

The experimental setup for measuring ice nucleation from H_2SO_4/H_2O particles is shown schematically in Figure 1. During the course of an experiment the aerosol passes through two temperature-controlled flow tubes, each cooled with methanol using Neslab circulating refrigerators. The first tube is used to set the composition of the aerosol and will be referred to as the conditioning region. For sulfuric acid experiments, the conditioning region is approximately 3.8 cm in diameter and 56 cm in length, providing a residence time of ~11 s. The aerosol is monitored in the second tube using FTIR spectroscopy. This tube is referred to as the observation region. The observation region is approximately 2.5 cm in diameter and 63 cm in length, providing a residence time of ~5 s.

Sulfuric acid particles are generated by atomizing a 96.1 wt% sulfuric acid solution. The bulk solution is fed into the atomizer (TSI 3076) using a Harvard apparatus syringe pump. On the basis of scanning mobility particle sizer measurements

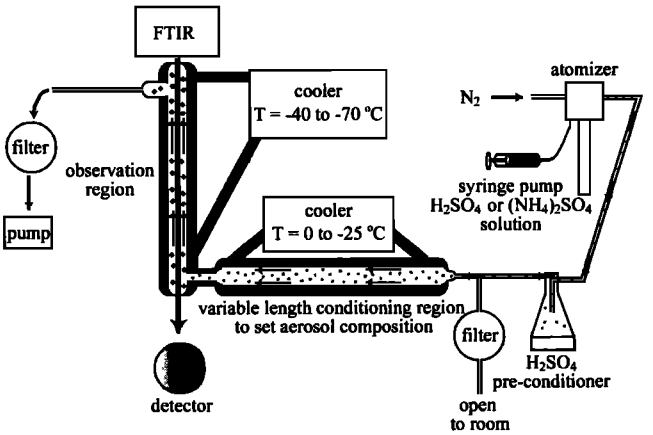

Figure 1. Experimental setup for the H_2SO_4/H_2O aerosol measurements. Submicrometer aerosol is generated using a TSI atomizer. The aerosol composition is then set using a sulfuric acid bath preconditioner and the conditioning region of the flow tubes. Ice nucleation is measured using Fourier transform infrared spectroscopy (FTIR) in the observation region. A similar setup was used for the $(NH_4)_2SO_4/H_2O$ aerosol measurements.

in our laboratory, we determine that the atomizer produces ~10^7 particles cm^{-3} with a mean droplet diameter of 0.3 μm and a geometric standard deviation of less than 2. The sulfuric acid particles pass over a sulfuric acid bath of desired concentration to add water to the particles, thus preconditioning the aerosol. The aerosol is then introduced into the flow tube system, where its final composition is reached in the conditioning region, and ice nucleation is measured in the observation region. In going from the atomizer to the observation region, the particles take up a significant amount of water, increasing the median diameter to ~0.55 μm; the median size may even be slightly larger due to particle coagulation. However, the largest particles in the size distribution (> 4 μm) are expected to settle out of the aerosol flow prior to reaching the observation tube.

Prior to introduction of the aerosol, the conditioning region is exposed to a counter flow of humidified nitrogen, coating the tube walls with ice. A simultaneous counter flow of dry nitrogen through the observation region ensures that only the conditioning region is coated with ice. By controlling the temperature of the ice-coated conditioning region, the water vapor pressure within this region is known. The aerosol is then sent through the conditioning region. If the aerosol is able to reach equilibrium with temperature and water vapor, the aerosol will have a well-defined composition, calculated using the Aerosol Inorganics Model (AIM) [*Carslaw et al.*, 1995; *Clegg et al.*, 1998a; *Clegg et al.*, 1998b; *Clegg et al.*, 2000 (available at http: www.uea.ac.uk/~e770/aim.html)].

To ensure that we do indeed have an accurate knowledge of water vapor in the tubes, we have monitored water vapor in the conditioning tube using an EdgeTech Dew Point II chilled mirror hygrometer. For this experiment, a flow of dry nitrogen is sent through the ice-coated flow tube, and water vapor is measured using the hygrometer at the exit of the observation region. Measurements at multiple temperatures confirm that ice does, in fact, coat the walls of the conditioning tube and that a constant water vapor pressure is

present in the tube. FTIR measurements of the aerosol, discussed below, indicate that the aerosol reaches equilibrium in the conditioning region and remains at this composition under appropriate flow conditions.

2.2. Ammonium Sulfate

For the ammonium sulfate experiments, higher vapor pressures of water caused excessive plugging at the junction of the flow tubes. For this reason and because of difficulty reaching equilibrium in the conditioning tube, the experimental setup shown in Figure 1 was modified for the ammonium sulfate ice nucleation measurements. The ammonium sulfate setup differs from that of sulfuric acid in several significant ways. First, rather than one conditioning tube, either two or three tubes were used, thereby extending the conditioning region to as much as 2 m. This addition gives the aerosol more time to reach equilibrium in the conditioning region, up to 60 s depending on flow rate. The observation tube was also shortened to 38 cm, decreasing the time allowed for loss of water from the particles to the cold flow tube walls. A transition tube was also added to the system, with one end of the tube at the conditioning temperature and the other end at the observation temperature. In doing this, the temperature drop from the conditioning to observation region now occurs in this transition region, and so water vapor condensation due to the temperature drop occurs on a very broad section of the flow tube (~5 cm diameter), decreasing the probability of plugging. This design also gives time for the aerosol to reach the observation temperature. Temperature measurements in the aerosol flow in the observation region indicate that the aerosol flow does reach the observation tube temperature. Finally, to further decrease the probability of plugging, the junctions between the tubes were increased from ~0.63 cm to ~2.5 cm diameter.

The bulk solution used for the ammonium sulfate studies was a 27 wt% ammonium sulfate solution made from crystalline ammonium sulfate (Fisher, 99.8% assay) and distilled water. Generating an aerosol using an ammonium sulfate solution yields less sulfate mass than generating an aerosol from sulfuric acid. This results because the ammonium sulfate solution in the syringe pump is initially only 27 wt%, while the sulfuric acid bulk solution is 96 wt%. Therefore to increase the mass produced by the atomizer, the syringe pump flow rate was increased. The extent to which this changed the size distribution was not quantified. The ammonium sulfate solution aerosol passes over the sulfuric acid bath to add or remove water, depending on the desired aerosol concentration. The aerosol is then introduced into the flow tube system where the final composition is reached and ice measurements are taken. As was the case for the H_2SO_4/H_2O system, aerosol composition is calculated on the basis of the temperature of the conditioning tube using the Aerosol Inorganics Model [*Carslaw et al.*, 1995; *Clegg et al.*, 1998a; 1998b; 2000 (available at http:www.uea.ac.uk/~e770/aim.html)].

2.3. Temperature Measurements

All flow tubes are jacketed to allow for a circulating methanol bath. Temperatures are measured using three thermistors in the conditioning region and five thermistors in the observation region. The thermistors were calibrated against a reference temperature measurement to ± 0.2°C over the temperature range studied. The thermistors are placed both in the coolant and in the aerosol flow. Temperature was recorded from each thermistor every 2-3 s and these measurements were averaged for each freezing point measurement. For the sulfuric acid solution experiments, the uncertainty in the temperature calibration (0.2°C) combined with one standard deviation for all of the thermistors in the conditioning region was always ≤ 0.4°C. This uncertainty is used to determine uncertainty in composition using the AIM thermodynamic model. The uncertainty in the temperature calibration combined with one standard deviation for all thermistors in the observation region for these measurements was always ≤ 1.1°C. This uncertainty corresponds to the uncertainty in the freezing point measurement and is shown as temperature error bars in later figures. Freezing point measurements for the ammonium sulfate solutions showed similar results. The calibration uncertainty combined with one standard deviation for the ammonium sulfate solution measurements was always ≤ 0.8°C in the conditioning region. This uncertainty is used to produce error bars for ammonium sulfate compositions. The uncertainty in the temperature calibration combined with one standard deviation for all thermistors in the observation region was always ≤ 0.6°C. This uncertainty is used to produce all temperature error bars for ammonium sulfate figures.

2.4. Determining Composition

For our method of determining composition to be successful, two requirements must be met. First, the aerosol must reach equilibrium in the conditioning region, and second, the aerosol must retain this composition in the observation region. In an effort to meet these conditions, we conducted experiments with a high number density of particles, thereby increasing the amount of water in the condensed phase relative to that in the gas phase. This diminished the effect of the excess gas phase water condensing onto the aerosol at the point of the temperature drop. For sulfuric acid the ratio of condensed phase to gas phase water was between 10 and 30 in the conditioning region for all experiments. Because we did not quantify the size distribution for the ammonium sulfate aerosol, we cannot determine the amount of condensed phase water in these experiments, although we expect similar condensed phase to gas phase ratios. To determine if we attained these conditions, we ran sulfuric acid and ammonium sulfate aerosol through the flow tubes at various flow rates and monitored aerosol composition using FTIR spectroscopy. For these tests, the conditioning region was set to produce a solution aerosol of desired composition, and the observation region was set to -39°C. For H_2SO_4/H_2O aerosol, flow tests were conducted for one high weight percent and one low weight percent composition. For $(NH_4)_2SO_4/H_2O$ aerosol, flow tests were run prior to each ice nucleation experiment.

For both H_2SO_4/H_2O and $(NH_4)_2SO_4/H_2O$ we observed three flow regimes. Figure 2 shows infrared spectra for the aerosol in all three regimes for ammonium sulfate, with the approximate locations of relevant peaks labeled. Flows of 1.3 liters per minute and 1.7 liters per minute are indicative of the slow flow regime. In this regime, the concentration of the aerosol varies greatly with flow rate, and the large sulfate stretch relative to the OH stretch indicates that the particles are very concentrated. This results because while the flow is

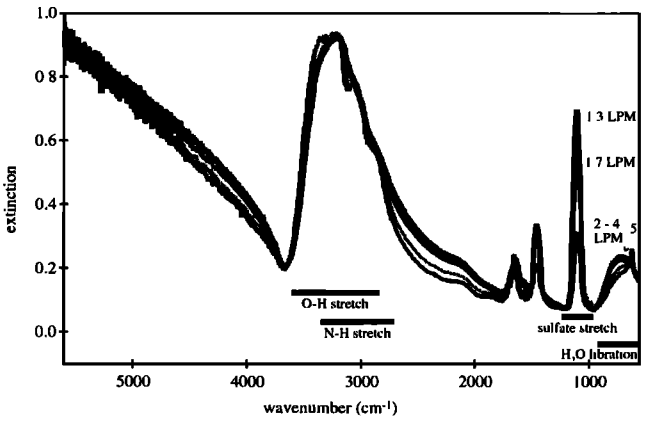

Figure 2. Infrared spectra of ammonium sulfate solution aerosol, with some of the major features identified. The spectra demonstrate three flow regimes for our experimental setup. In the slow flow regime (1.3 and 1.7 liters per minute (LPM)) the aerosol does not reach equilibrium in the tubes and is very concentrated, indicated by the high sulfate stretch to OH stretch ratio. In the intermediate flow regime (2, 3, and 4 LPM) the sulfate stretch to OH stretch ratio remains constant, indicating that the composition is constant. In this regime the aerosol is at equilibrium, and composition can be determined using a thermodynamic model. In the fast flow regime (5 LPM) the sulfate stretch to OH stretch ratio begins to decrease, and the H_2O libration stretch begins to increase (designated with an arrow), indicating nonequilibrium conditions. Spectra are not to scale.

sufficiently slow for the aerosol to reach equilibrium in the conditioning region, it is so slow that there is also significant water transfer from the conditioned aerosol to the cold observation tube walls, thus concentrating the aerosol in the observation region. An increase in flow puts the aerosol in the intermediate flow regime. Here, the flow is sufficiently slow for the aerosol to reach equilibrium in the conditioning region, and sufficiently fast for the aerosol to remain at this composition in the observation region. In this regime, a change in flow does not result in a change of aerosol composition. For example, in the experiment shown, flows of 2 LPM, 3 LPM, and 4 LPM resulted in essentially identical IR spectra, indicating a constant composition throughout. In this regime, we assume that the aerosol has been able to reach equilibrium in the conditioning region, and composition is calculated using the AIM thermodynamic model. In contrast, increasing the flow further results in particles which do not reach equilibrium in the conditioning region. As in the slow flow regime, composition varies with flow rate in the fast flow regime. In Figure 2, for example, a flow of 5 LPM yielded a spectrum which had a smaller sulfate stretch relative to the OH stretch and an enhanced H_2O libration, indicating the aerosol was slightly more dilute than in the equilibrium regime. The libration enhancement is indicated with an arrow in the figure.

2.5. Measuring Crystallization

After ensuring an accurate determination of aerosol composition, an aerosol infrared spectrum is taken at temperatures well above the freezing temperature, where no solids are present in the particles. The temperature of the observation region is then incrementally cooled, while the temperature of the conditioning region remains constant, and the phase of the aerosol is monitored using FTIR spectroscopy. Near the freezing point, the observation tube is cooled in ~1°C increments until ice formation is observed. Small spectroscopic changes can result when cooling the aerosol due to the temperature dependence of the optical constants [*Niedziela et al.*, 1998]. However, no spectroscopic changes are observable when there are only small temperature changes (< 2°C) unless freezing is initiated. Spectral subtractions of the aerosol at similar temperatures therefore yield only noise unless freezing has begun.

When the aerosol reaches the freezing point for ice, several distinct changes occur in the infrared for H_2SO_4/H_2O [*Bertram et al.*, 1996] and for $(NH_4)_2SO_4/H_2O$ aerosol [*Cziczo and Abbatt*, 1999]. For H_2SO_4/H_2O the OH-stretching region, which has a maximum at ~ 3300 cm^{-1}, shifts to slightly lower frequencies, while the H_2O stretch, centered near 800 cm^{-1}, shifts to slightly higher frequencies. Similar shifts occur for $(NH_4)_2SO_4/H_2O$ aerosol. The temperature at which both of these noted spectral changes are first clearly visible in the infrared is used as the freezing point measurement. We estimate that approximately 5 - 10% of the particle mass must freeze for this to be clearly visible in the infrared for our system. In Figure 3, a 12 wt% ammonium sulfate solution aerosol is incrementally cooled from -39 °C to -45 °C. The spectra remain unchanged (curve a; overlaid) from -39 °C to -43 °C, indicating that the particles remain aqueous. The spectrum at -45°C (curve b) shows the aerosol after a significant amount of ice has formed. The spectrum at -44 °C, the onset of ice nucleation, has been omitted for clarity. In conjunction with ice formation the N-H stretch at 3050 cm^{-1} also becomes more defined. It is unclear if this results from the simultaneous crystallization of $(NH_4)_2SO_4$ or from the enhanced concentration of the remaining droplets.

3. Results and Discussion

3.1. Sulfuric Acid

Freezing measurements were systematically carried out for pure water and for 15-24 wt% sulfuric acid. These data are

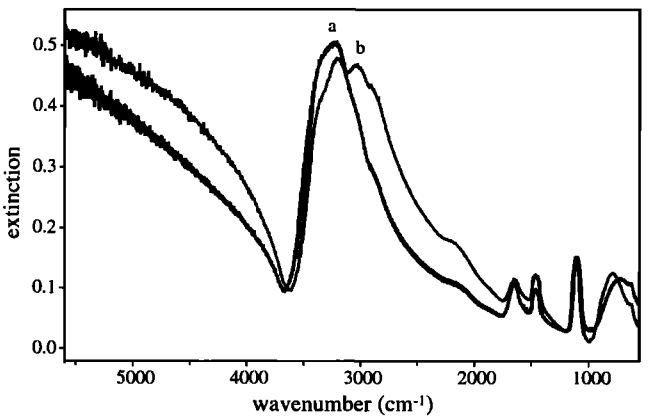

Figure 3. Infrared spectra representative of an ice nucleation experiment. In this figure, a 12 wt% ammonium sulfate solution aerosol is incrementally cooled from -39°C to -43°C (overlaid, curve a) with no change in the infrared spectra, indicating that ice has not yet nucleated. At -45°C (curve b) a significant amount of ice has formed, as indicated by the shifts in peaks at ~3300 cm^{-1} and ~800 cm^{-1}.

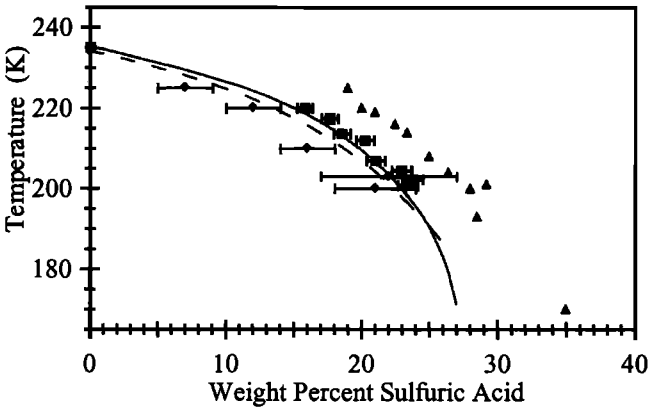

Figure 4. Ice formation temperatures from H_2SO_4/H_2O aerosol as a function of weight percent. The squares designate the data from this study; the triangles designate the data from *Bertram et al.* [1996]; the diamonds designate the data from *Cziczo and Abbatt* [1998]; the solid line designates the data from *Koop et al.* [1998]; and the dashed line designates the data of *Chen et al.* [2000].

plotted as squares as a function of sulfuric acid weight percent in Figure 4, together with previous measurements of ice nucleation from H_2SO_4/H_2O particles [*Bertram et al.*, 1996; *Cziczo and Abbatt*, 1998; *Koop et al.*, 1998, *Chen et al.*, 2000]. Ice nucleation from pure water droplets is apparent at 235 K, in good agreement with previous studies. The composition range investigated in our study was limited by our refrigerator's cooling capabilities on the high composition end and by excessive water vapor causing plugging on the low composition end. Our results indicate that freezing temperature is strongly dependent on aerosol composition. This agrees well with the data of *Koop et al.* [1998], shown as a solid curve in the figure, and moderately well with the data of *Chen et al.* [2000], shown as a dashed curve.

In the *Koop et al.* [1998] study, aerosols were produced with a nebulizer and deposited on a quartz plate. Freezing and melting were then monitored using an optical microscope, and the corresponding temperatures for these phase changes were recorded for more than 1200 individual particles. The curve in Figure 4 is the fit to their median freezing temperatures for a number of particles with like compositions [from *Koop et al.* [1998], Table 1]. In the *Chen et al.* [2000] studies, pure sulfuric acid particles with ≤ 0.1 μm diameter were generated, exposed to water vapor, and monitored in a continuous flow thermal diffusion chamber. The dashed curve in Figure 4 is based on a fit to their data. In the *Bertram et al.* [1996] study, shown as triangles in the figure, and the *Cziczo and Abbatt* [1998] study, shown as diamonds, freely floating, submicrometer H_2SO_4/H_2O particles were cooled in a flow tube system and monitored using FTIR spectroscopy. Both of these groups reported the onset of ice formation in the aerosol. Our results fall between the measurements of *Bertram et al.* [1996] and *Cziczo and Abbatt* [1998], which were done under similar conditions. Because all three experiments used like-sized aerosol and each group reports the onset of ice nucleation, the cause for the discrepancy is unclear.

Our results agree best with the studies which do not use FTIR spectroscopy to determine freezing temperatures. The freezing point depression is ≥ 39°C for all of our H_2SO_4/H_2O measurements, with a supercooling of ~44°C to nearly 55°C for the composition range of 15.8-23.8 wt%. However, we do not observe the extent of supercooling that *Koop et al.* [1998] or *Chen et al.* [2000] measured. Our measured freezing temperatures are systematically higher by an average of ~2.5°C compared to *Koop et al.* [1998] and ~5°C compared to *Chen et al.* [2000]. These differences can be explained qualitatively by a number of arguments. First, the differences could be due solely to the uncertainties in the measurements. This seems unlikely, however, since our measurements yield higher freezing temperatures for all compositions monitored. The discrepancy with the *Chen et al.* [2000] data may be attributed to size differences, as we are measuring larger particles and would therefore expect to observe higher freezing temperatures, in agreement with homogeneous nucleation theory.

Our particles are smaller than those in the *Koop et al.* [1998] studies, and so size cannot explain the discrepancy between these two data sets. Rather, this discrepancy may be explained on the basis of the difference in freezing temperature determination. While we report the onset of ice nucleation for an ensemble of particles, *Koop et al.* [1998] measure each freezing point independently and report the median freezing temperature. Their technique enables the measurement of a range of freezing temperatures, in which ice nucleation is first apparent at temperatures slightly higher than the median temperature of the freezing point line. They see a total freezing point range of ~4°C, due to the stochastic nature of the freezing process. Because we are reporting the onset of freezing, it is not surprising that we fall on the upper end of the range of their freezing temperature data. For a few of our experiments we continued to cool the aerosol after the onset of ice nucleation. These measurements showed further ice formation at lower temperatures, similar to what *Koop et al.* [1998] observed. In our case, however, this may result from the relatively large spread in our size distribution and the volume dependence of freezing. For the H_2SO_4/H_2O system we did not conduct any systematic tests to determine the temperature at which freezing was complete, and so we are unable to provide a range of freezing temperatures for our range of particle sizes.

The freezing point data can be used to determine the humidity conditions necessary for ice formation in the atmosphere. The parameter most often used in cloud microphysical models is the temperature-dependent critical ice saturation ratio, $S(T)$, defined as

$$S(T) = \frac{P_{H_2O}}{P(T,ice)}, \quad (1)$$

where P_{H_2O} is the partial pressure of water at a specified temperature and $P(T,ice)$ is the vapor pressure of water over ice at that same temperature. Figure 5 shows the critical ice saturation ratio as a function of temperature, based on our measurements (circles), as well as calculated ice saturation ratios for three theoretical cases, based on a kinetic model constrained by the data of *Koop et al.* [1998; *Tabazadeh et al.*, 2000]. The model calculations have been performed for two scenarios in our experimental apparatus. In the first calculation (dashed line in Figure 5) the model assumes a monodisperse size distribution with 0.5 μm diameter particles, and ice supersaturations are calculated for 5% of the particles to nucleate ice with a freezing rate of $J = 1\ s^{-1}$. The model clearly overestimates our saturation ratios using these parameters. However, we do not have a monodisperse size

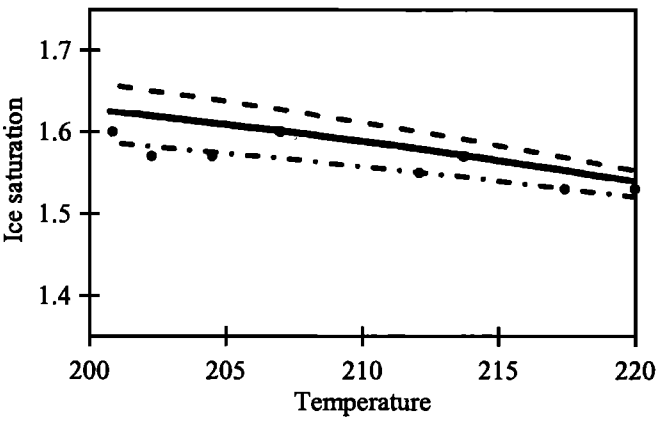

Figure 5. Ice saturation ratio for H_2SO_4/H_2O aerosol as a function of temperature. The circles represent the measured ice saturation ratio for this work. The dashed line represents calculated ice saturation ratios based on a kinetic model [*Tabazadeh et al.*, 2000]. The model assumes a monodisperse size distribution with 0.5 μm diameter particles, and ice supersaturations are calculated for 5% of the particles to nucleate ice. The solid line represents calculations based on the same model, in which the necessary ice saturation ratio is determined for 5% of the aerosol mass to freeze, assuming that only the largest particles freeze. Calculations are based on a lognormal size distribution, assuming a count median diameter of 0.5 μm and $\sigma = 1.8$. Finally, the dashed-dotted line represents S for 1% of the largest particles to freeze.

distribution in our experiment, rather we have a relatively broad size distribution, as noted in section 2. If we consider this size distribution and change the model parameters, we can determine the ice supersaturation necessary for 5% of our aerosol mass to freeze, with all of the nucleation occurring in the largest particles. The result of this calculation is shown in Figure 5 as a solid line. Clearly, this fits our data much better. Finally, we calculate S for 1% of the largest particles to freeze, shown as a dashed-dotted line in Figure 5. The calculations for 1% and 100% of the largest particles to freeze bracket our measured ice saturation ratios. This indicates that the "onset" of freezing that we report is probably for the largest particles in our size distribution and that the additional freezing at lower temperatures is for the smaller particles in the distribution. The good fit also indicates that our data for freely floating aerosol is quantitatively consistent with that of *Koop et al.* [1998] for particles on a quartz plate.

3.2. Ammonium Sulfate

Ice freezing data from experiments on 0 to 40 wt% ammonium sulfate solution aerosol are shown as solid squares in Figure 6. The observed freezing temperatures over this composition range are much higher than the freezing temperatures for sulfuric acid aerosols of similar weight percent. Also included in this figure are other reported freezing points. *Cziczo and Abbatt* [1999] (triangles) used a similar flow tube and FTIR technique and found freezing temperatures higher than ours, especially at high ammonium sulfate weight percent. Their experiment differs from ours in several ways, most significantly in the method used to determine aerosol composition. In contrast to our approach of assuming equilibrium in the conditioning tube, *Cziczo and Abbatt* [1999] use an infrared calibration to determine aerosol composition. While it is unclear at present if this difference is the cause for the measurement discrepancy, it may be at least partially responsible. A fit to the data of *Bertram et al.* [2000] is shown as a dashed curve [from *Bertram et al.* [2000], Table 1], and a fit to the data of *Chen et al.* [2000] is shown as a dashed-dotted curve. The *Bertram et al.* [2000] studies employ differential scanning calorimetry and optical microscopy. The data are shown as a least squares fit to both the median freezing temperatures obtained in the optical microscope experiments and the temperatures at which 50% of the particle mass freezes in the differential scanning calorimetry experiments. The *Chen et al.* [2000] studies use a continuous flow thermal diffusion chamber. These studies report freezing temperatures for 1% of monodisperse particles (0.2 μm) to freeze. Both studies show significantly greater supercooling than either of the aerosol flow tube studies.

Cloud physics models often represent the degree of supercooling of solution aerosol using the following expression:

$$\Delta T_{f,\mathrm{soln}} = T_{f,\mathrm{H_2O}} - T_{f,\mathrm{soln}} = \lambda \Delta T_m, \quad (2)$$

where $\Delta T_{f,\mathrm{soln}}$ is the freezing point depression for a solution at a given weight percent, $T_{f,\mathrm{H_2O}}$ is the freezing temperature of a pure water droplet of the same size and at the same nucleation rate as the solution droplet, $T_{f,\mathrm{soln}}$ is the freezing temperature of the solution droplet, ΔT_m is the bulk melting point depression for an ammonium sulfate solution at the given weight percent [*Clegg et al.*, 1998a; 2000 (available at: http: www.uea.ac.uk/~e770/aim.html)], and λ represents the relationship between the ice nucleation point depression in particles and the bulk melting point depression for salt solutions. The freezing and melting depressions and λ are all positively valued in this expression. A λ of 1.7 has been

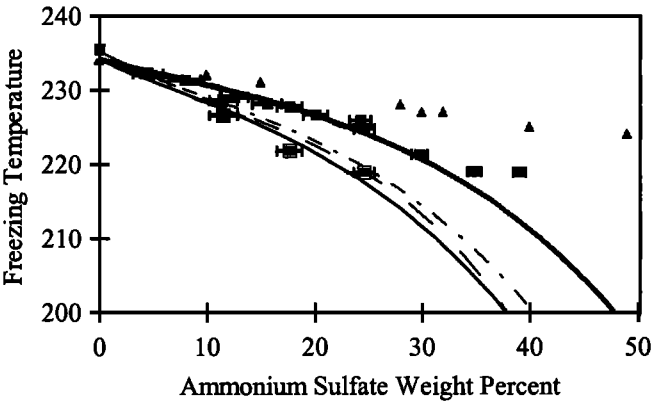

Figure 6. Ice formation temperatures from $(NH_4)_2SO_4/H_2O$ aerosol as a function of weight percent. The solid squares represent data for the onset of freezing for this study. The open squares represent complete freezing, also from this study. Both sets of data are fitted with the parameter λ, which represents the relationship between the nucleation and the melting point depressions. For the onset of freezing, $\lambda = 1.2$, shown as a thick solid curve; for complete freezing, $\lambda = 2.0$, shown as a thin solid curve. Other data are also presented. The triangles represent the work of *Cziczo and Abbatt* [1999]; the dashed curve represents the work of *Bertram et al.* [2000]; and the dashed-dotted curve represents the data of *Chen et al.* [2000].

suggested [*DeMott et al.*, 1994; *Sassen and Dodd*, 1988] for cirrus formation based on earlier measurements of the supercooling of various other salt solutions [*Rasmussen*, 1982]. *Chen et al.* [2000] have measured $\lambda = 1.75$ (dashed-dotted curve) for ice formation from ammonium sulfate solution aerosol, very close to this proposed value. *Cziczo and Abbatt* [1999] determine λ to be less than 1 based on their aerosol measurements. Using the current data, we calculate $\lambda = 1.2$ for the onset of ice formation, shown as the thick, solid curve fit to the data in Figure 6. Our determination of λ corresponds to an aerosol supercooling of just slightly greater than 39 °C.

For several compositions the aerosol was cooled further in an effort to measure complete ice formation. For these experiments the aerosol was cooled in 1°C increments, and additional ice formation was monitored. The temperature at which further cooling did not yield additional ice features in the infrared was chosen as the point at which the entire aerosol was frozen. These measurements yielded freezing temperatures that were 2°-6°C colder than the freezing onset temperatures. This spread in data is consistent with that reported by *Bertram et al.* [2000], in which the average temperature difference for 10% frozen relative to 90% frozen is 2.6 °C. The data for completely frozen aerosol are shown in Figure 6 as open squares. On the basis of only these three points we determine a new freezing point depression parameter of $\lambda = 2.0$, shown as a thin solid curve fit to the data, for complete freezing of the aerosol. These complete freezing points provide better agreement with the data of *Bertram et al.* [2000] and *Chen et al.* [2000]. While a solution aerosol is expected to have a constant value of λ, this value can only be determined precisely with size-dependent measurements of freezing temperatures. Because we measure a range of sizes simultaneously, we are unable to determine λ definitively, and so these two values for λ, 1.2 and 2.0, serve to provide a range for ammonium sulfate aerosol with a submicrometer median diameter and a broad size distribution.

Although our complete freezing data agree fairly well with the *Bertram et al.* [2000] and *Chen et al.* [2000] studies, our onset freezing temperatures are much higher. We can employ the same arguments as for sulfuric acid solution aerosol to explain these discrepancies. Namely, the largest particles in our size distribution are larger than the particles measured by *Chen et al.* [2000], and so homogeneous nucleation theory predicts freezing at higher temperatures. In contrast, *Bertram et al.* [2000] measure freezing in larger particles. However, they report freezing for a larger fraction of particles frozen. As noted above, when we measured complete freezing, our freezing temperatures dropped significantly.

An alternative explanation can be obtained from the data of *Chen et al.* [2000]. They measure a relatively constant λ for 0.1%, 1%, and 10% particles frozen for sulfuric acid solutions. In contrast, λ is dependent on the fraction of particles frozen for ammonium sulfate solutions. Specifically, *Chen et al.* [2000] determine $\lambda \approx 1$ for the onset (0.1%) of nucleation, a value much closer to our onset measurements, and a much larger $\lambda \approx 1.75$ for greater freezing (1%). For the broad size distributions in our measurements ($\sigma \approx 1.8$), 0.1% of the particle number can account for a large fraction of the particle mass; for example, if all of the particles in the size range of 3.2-4.0 μm freeze (0.1% of the particle number), this corresponds to ~6% of the particle mass. FTIR measurements are sensitive to mass, not number, and so this may greatly affect our freezing temperature observations.

Ice saturation ratios are also determined as a function of temperature for ammonium sulfate solution aerosols. These data are shown in Figure 7, along with our data for sulfuric acid aerosol. In the figure, the solid circles represent the sulfuric acid data, and the open circles represent the ammonium sulfate data. While ammonium sulfate aerosols froze at higher temperatures than sulfuric acid aerosols of similar weight percent, they did not have a significantly lower saturation ratio than predicted by the trend for sulfuric acid. Specifically, with the exception of the two data points at 219 K, S was nearly constant, with a value of 1.48 ± 0.01. The two values near 219 K, the most concentrated aerosol monitored, fell well below $S = 1.48$. Beyond these compositions (~40 weight percent), ammonium sulfate solutions become metastable with respect to crystallization to solid ammonium sulfate. It is unclear if this is the cause for the lower ice saturations, or if the sudden drop in the measured S at 219 K is a problem with measuring ice nucleation near this region. Another possibility is that the para-to-ferro phase transition for ammonium sulfate, which occurs at 223 K, may affect the ice nucleation point.

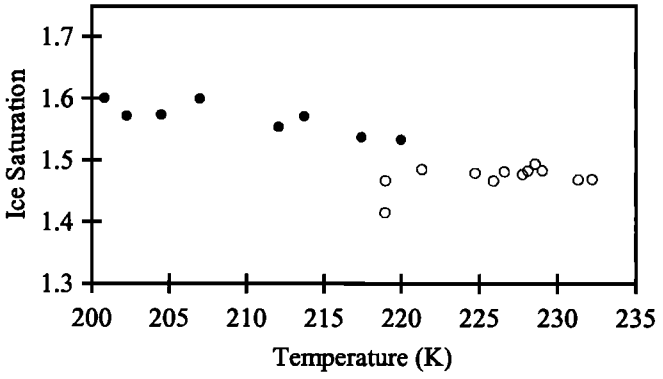

Figure 7. Ice saturation ratio, S, for H_2SO_4/H_2O (solid circles) and $(NH_4)_2SO_4/H_2O$ (open circles) aerosol as a function of temperature. The ammonium sulfate data do not differ significantly from the sulfuric acid data, indicating that the presence of fully ammoniated sulfate aerosols does not greatly affect freezing temperatures.

4. Conclusions and Atmospheric Implication

Ice nucleation temperatures have been measured in H_2SO_4/H_2O and $(NH_4)_2SO_4/H_2O$ aerosol. We measure freezing temperatures of 220 K to 200 K for H_2SO_4/H_2O aerosol with compositions of 16 to 24 weight percent, respectively. This corresponds to an equilibrium ice saturation ratio of approximately $S = 1.53$ to $S = 1.6$ over this same temperature range. This agrees well with field data of ice saturation measured near the leading edge of a wave cloud [*Jensen et al.*, 1998], which reports $S = 1.6$ at 209 K. For $(NH_4)_2SO_4/H_2O$ aerosol, freezing temperatures of 232 K to 219 K are measured for aerosol with compositions of 4 to 39 weight percent, respectively. Equilibrium ice saturation for ammonium sulfate aerosol yielded a more constant value of approximately $S = 1.48$ over this temperature range.

The high values of ice saturation for both sulfuric acid and ammonium sulfate solutions indicate that high humidities

and/or low temperatures must be experienced for ice nucleation in the atmosphere. Because of the high ice saturation necessary for homogenous nucleation, cirrus particles may form by an alternative pathway. Our data suggest that the saturation ratio increases as temperature decreases in the temperature range studied, from approximately 1.53 at 220 K to 1.6 at 200 K. This agrees in form with the data reported by *Koop et al.* [1998]; however, in their paper the saturation ratios reported were somewhat higher. While we have only measured nucleation down to 200 K, we assume, based on the trend for both the data and the model, that S will continue to increase as temperature decreases. Further, we expect that S will exceed 1.6 below 200 K for submicrometer aerosol. The high values of S required for ice formation has implications for cloud formation. If ice polar stratospheric clouds were to form from sulfuric acid solution aerosol, these data suggest that large ice saturations would be required, consistent with observations of 3°-4°C supercooling for ice PSCs.

Acknowledgments. This work was supported by NASA-SASS and NSF-ATM. AJP would like to acknowledge the EPA STAR Fellowship Program for funding. The authors would like to thank A. Tabazadeh for the use of her model, Paul DeMott for helpful input, and Scot Martin and all of the other participants at the AGU post-session roundtable meeting for access to yet unpublished data and for many helpful discussions.

References

Bertram, A. K., D. D. Patterson, and J. J. Sloan, Mechanisms and temperatures for the freezing of sulfuric acid aerosols measured by FTIR extinction spectroscopy, *J. Phys. Chem.*, *100*, 2376-2383, 1996.

Bertram, A. K., T. Koop, L. T. Molina, and M. J. Molina, Ice formation in $(NH_4)_2SO_4$-H_2O particles, *J. Phys. Chem. A*, *104*, 584-588, 2000.

Carslaw, K. S., S. L. Clegg, and P. Brimblecombe, A thermodynamic model of the system HCl-HNO_3-H_2SO_4-H_2O, including solubilities of HBr, from <200 to 328 K, *J. Phys. Chem.*, *99*, 11,557-11,574, 1995.

Charlson, R. J., S. E. Schwartz, J. M. Hales, R. D. Cess, J. A. Coakley, J. E. Hansen, and D. J. Hofmann, Climate forcing by anthropogenic aerosols, *Science*, *255*, 423-430, 1992.

Chelf, J. H., and S. T. Martin, Homogeneous ice nucleation in aqueous ammonium sulfate aerosol particles, *J. Geophys. Res.*, in press, 2000.

Chen, Y., P. J. DeMott, S. M. Kreidenweis, D. C. Rogers, and D. E. Sherman, Ice formation by sulfate and sulfuric acid aerosol particles under upper tropospheric conditions, *J. Atmos. Sci.*, *57*, 3752-3766, 2000.

Clapp, M. L., R. F. Niedziela, L. J. Richwine, T. Dransfield, R. E. Miller, and D. R. Worsnop, Infrared spectroscopy of sulfuric acid/water aerosols: Freezing characteristics, *J. Geophys. Res.*, *102*, 8899–8907, 1997.

Clegg, S. L., P. Brimblecomb, and A. Wexler, A thermodynamic model of the system H^+-NH_4^+-SO_4^{2-}-NO_3^--H_2O at tropospheric temperatures, *J. Phys. Chem. A*, *102*, 2137-2154, 1998a.

Clegg, S. L., P. Brimblecomb, and A. Wexler, A thermodynamic model of the system H-NH_4-Na-SO_4-NO_3-Cl-H_2O at 298.15 K, *J. Phys. Chem. A*, *102*, 2155-2171, 1998b.

Clegg, S.L., P. Brimblecomb, and A. Wexler, Aerosol Inorganics Model (AIM), 2000.

Cziczo, D. J., and J. P. D. Abbatt, Deliquescence, efflorescence, and supercooling of ammonium sulfate aerosols at low temperature, *ES Trans. AGU Fall Meet. Suppl.*, *79*, F108, 1998.

Cziczo, D. J., and J. P. D. Abbatt, Deliquescence, efflorescence, and supercooling of ammonium sulfate aerosols at low temperature: Implications for cirrus cloud formation and aerosol phase in the atmosphere, *J. Geophys. Res.*, *104*, 13,781-13,790, 1999.

DeMott, P. J., and D. C. Rogers, Freezing nucleation rates of dilute solutions droplets measured between -30°C and -40°C in laboratory simulations of natural clouds, *J. Atmos. Sci.*, *47*, 1056-1064, 1990.

DeMott, P. J., M. P. Meyers, and W. R. Cotton, Parameterization and impact of ice initiation processes relevant to numerical model simulations of cirrus clouds, *J. Atmos. Sci.*, *51*, 77-90, 1994.

Gable, C. M., H. F. Betz, and S. H. Maron, Phase equilibria of the system sulfur trioxide-water, *J. Am. Chem. Soc.*, *72*, 1445-1448, 1950.

Hu, J. H., and J. P. D. Abbatt, Reaction probabilities for N_2O_5 hydrolysis on sulfuric acid and ammonium sulfate, *J. Phys. Chem. A*, *101*, 871-878, 1997.

Imre, D., J. Xu, and A. C. Tridico, Phase transformation in sulfuric acid aerosols: Implications for stratospheric ozone depletion, *Geophys. Res. Lett.*, *24*, 69-72, 1997.

Jensen, E. J., et al., Ice nucleation processes in upper tropospheric wave-clouds observed during SUCCESS, *Geophys. Res. Lett.*, *25*, 1363-1366, 1998.

Koop, T., H. P. Ng, L. T. Molina, and M. J. Molina, A new optical technique to study aerosol phase transitions: The nucleation of ice from H_2SO_4 aerosols, *J. Phys. Chem. A*, *102*, 8924-8931, 1998.

Lary, D. J., A. M. Lee, M. J. Newchurch, M. Pirre, and J. B. Renard, Carbon aerosols and atmospheric photochemistry, *J. Geophys. Res.*, *102*, 3671-3682, 1997.

Martin, S. T., Phase transformations of the ternary system $(NH_4)_2SO_4$-H_2SO_4-H_2O and the implications for cirrus cloud formation, *Geophys. Res. Lett.*, *25*, 1657-1660, 1998.

Martin, S. T., D. Salcedo, L. T. Molina, and M. J. Molina, Phase transformations of micron-sized H_2SO_4/H_2O particles studied by infrared spectroscopy, *J. Phys. Chem. B*, *101*, 5307-5313, 1997.

Niedziela, R. F., M. L. Norman, R. E. Miller, and D. R. Worsnop, Temperature- and composition-dependent infrared optical constants for sulfuric acid, *J. Phys. Chem. A*, *102*, 6477-6484, 1998.

Ohtake, T., Freezing points of H_2SO_4 aqueous solutions and formation of stratospheric ice clouds, *Tellus*, *45 Ser. B*, 138-144, 1993.

Onasch, T. B., R. L. Siefert, S. D. Brooks, A. J. Prenni, B. Murray, M. A. Wilson, and M. A. Tolbert, Infrared spectroscopic study of the deliquescence and efflorescence of ammonium sulfate aerosol as a function of temperature, *J. Geophys. Res.*, *104*, 21,317-21,326, 1999.

Pandis, S. N., A. S. Wexler, and J. H. Seinfeld, Dynamics of tropospheric aerosols, *J. Phys. Chem.*, *99*, 9646-9659, 1995.

Rasmussen, D.H., Thermodynamic and nucleation phenomena: A set of experimental observations, *J. Cryst. Growth*, *56*, 56-66, 1982.

Sassen, K., and G. Dodd, Homogeneous nucleation rate for highly supercooled cirrus cloud droplets, *J. Atmos. Sci.*, *45*, 1357-1369, 1988.

Solomon, S., S. Borrmann, R. R. Garcia, R. Portmann, L. Thomason, L. R. Poole, D. Winker, and M. P. McCormick, Heterogeneous chlorine chemistry in the tropopause region, *J. Geophys. Res.*, *102*, 21,411-21,429, 1997.

Tabazadeh, A., and O. B. Toon, The role of ammoniated aerosols in cirrus cloud formation, *Geophys. Res. Lett.*, *25*, 1379-1382, 1998.

Tabazadeh, A., S. T. Martin, and J. -S. Lin, The effect of particle size and nitric acid uptake on the homogeneous freezing of aqueous sulfuric acid particles, *Geophys. Res. Lett.*, *27*, 1111-1114, 2000.

Talbot, R. W., J. E. Dibb, and M. B. Loomis, Influence of vertical transport on free tropospheric aerosols over the central USA in springtime, *Geophys. Res. Lett.*, *25*, 1367-1370, 1998.

Timmermans, J., *Physico-Chemical Constants of Binary Systems in Concentrated Solutions*, 619-620 pp., Wiley Intersci., New York, 1960.

Xu, J., D. Imre, R. McGraw, and I. Tang, Ammonium sulfate: Equilibrium and metastability phase diagrams from 40°C to -50°C, *J. Phys. Chem.*, *102*, 7462-7469, 1998.

Zhang, R., P. J. Wooldridge, J. P. D. Abbatt, and M. J. Molina, Physical chemistry of the H_2SO_4/H_2O binary system at low temperatures: Stratospheric implications, *J. Phys. Chem.*, *97*, 7351-7358, 1993.

S.D. Brooks, A.J. Prenni, M.A. Tolbert, and M.E. Wise, University of Colorado, Campus Box 216, Boulder, CO 80309. (sarah.brooks@colorado.edu; tony@aerosol.atmos.colostate.edu; tolbert@spot.colorado.edu; matthew.wise@colorado.edu)

(Received March 1, 2000; revised June 21, 2000; accepted July 9, 2000.)